FINAL REPORT NASA GRANT NAG-1-971
(January 1, 1989 - January 31, 1991)

P 27

MICRO-MECHANICAL ANALYSIS OF DAMAGE GROWTH AND FRACTURE IN DISCONTINUOUS FIBER REINFORCED METAL MATRIX COMPOSITES

June 10, 1991

Principal Investigator
James G. Goree
Centennial Professor
Department of Mechanical Engineering
Clemson University
Clemson, South Carolina 29634-0921

Graduate Assistant

David E. Richardson
Ph.D. Candidate in Engineering Mechanics

(NASA-CR-188206) MICRO-MECHANICAL ANALYSIS OF DAMAGE GROWTH AND FRACTURE IN DISCONTINUOUS FIBER REINFORCED METAL MATRIX COMPOSITES Final Report, 1 Jan. 1989 - 31 Jan. 1991 (Clemson Univ.) 27 p CSCL 11D G3/24

N91-24346

Unclas
0014962

ABSTRACT: This paper presents an experimental verification of a new two parameter fracture model based on the equivalent remote biaxial stresses (ERBS) developed by the authors. A detailed comparison is made between the new theory and the constant K_{IC} approach of Linear Elastic Fracture Mechanics (LEFM). Fracture is predicted through a failure curve representing the change in a variable fracture toughness K_C with the ERBS ratio B_E. The nonsingular term (T) in the series expansion of the near crack-tip transverse stress is included in the model. Experimental results for polymethyl methacrylate (PMMA) show that the theory can account for the effects of geometry on fracture toughness as well as indicate the initiation of crack branching. It is shown that the new criterion predicts failure for PMMA with a 95% confidence zone which is nearly three times smaller than that of the LEFM KIC approach.

Introduction

For many years the concept of a constant fracture toughness (K_{IC}), from Linear Elastic Fracture Mechanics (LEFM), has been used to predict failure in cracked bodies. Recently, however, researchers have pointed out that some of the basic assumptions of LEFM may not be accurate [1]. Others have found inconstencies in predicting fracture for some materials, both isotropic and anisotropic, from test results which satisfy the LEFM requirements for brittle plane strain behavior [2-3]. The purpose of this paper is to present some of the experimental test results from [4] that show the limitations of the constant K_{IC} failure criterion and support the new ERBS fracture model proposed in [4].

The ERBS concept is based on the fact that the near crack-tip stresses in any arbitrary coupon subjected to mode I loading with a load-free crack surface may be equated to those in an infinite biaxially loaded center-cracked panel of the same material and thickness and with a fixed crack length c^* (see Fig.

1). This is done by requiring that the stress intensity factors (K_I) and the constant terms (T) in the series expansion of near crack-tip stresses for both geometries be equal. For coupons of anisotropic material,

$$K_I=\sigma_y^{\infty}\sqrt{\pi c^*},$$

$$T=\sigma_x^{\infty}+\sigma_y^{\infty}(s_1 s_2).$$

Solving for σ_x^{∞} and σ_y^{∞} gives:

$$\sigma_x^{\infty}=\frac{-K_I}{\sqrt{\pi c^*}}Re(S_1 S_2)+T,$$

$$\sigma_y^{\infty}=\frac{K_I}{\sqrt{\pi c^*}}.$$

From these Equivalent Remote Biaxial Stresses (ERBS), the ERBS ratio (B_E) is defined as:

$$B_E=\frac{\sigma_x^{\infty}}{\sigma_y^{\infty}}=\frac{T}{K_I}\sqrt{\pi c^*}-RE(s_1 s_2). \qquad (1)$$

This ratio plays an integral role in the failure criterion. Here s_1 and s_2 are the positive roots of the characteristic equation [5]. For an isotropic material both roots are positive i ($i=\sqrt{-1}$).

The basic assumption of the ERBS fracture model is that failure in any planar arbitrary mode I coupon with an unloaded crack surface will be the same as that found in an "equivalent" infinite biaxially loaded center-cracked panel of the same material with a fixed crack length c^*. The failure of the infinite cracked panel with different remote loadings (Fig. 1) is

characterized through an ERBS curve, a graph representing the change in fracture toughness K_C with the ratio of the remote biaxial stresses B_E ($\sigma_x^\infty/\sigma_y^\infty$). K_C is a variable fracture toughness as opposed to the LEFM concept of a constant fracture toughness, K_{IC}.

To predict fracture in an arbitrary cracked coupon K_I and T must be found. The ERBS ratio (B_E) is then determined through equation 1, and from the ERBS curve K_C may be obtained for that particular coupon. K_C can be used to predict crack growth initiation just as K_{IC} in the LEFM approach.

Even though the ERBS curve represents failure of an infinite cracked panel, the curve need not be generated by fracture testing very large biaxially loaded cracked panels. Indeed, if this were the case the theory would have little practical use. Since differences in coupon geometry translate to changes in B_E, the ERBS curve may be generated by testing a variety of relatively simple coupon geometries (for example, pin-loaded edge-notched coupons). Each test represents only one point on the failure curve. A curve fit for a series of test results gives a mathematical expression for the shape of the ERBS curve.

Testing

To illustrate the similarities and differences between the LEFM and the ERBS failure criteria, and to demonstrate the accuracy of the ERBS approach, a series of fracture tests were conducted on various coupons of polymethyl methacrylate (PMMA). The 12.7 mm thick PMMA used in this study meets the plane strain

thickness requirement specified in the ASTM Standard for Plane-Strain Fracture Toughness of Metallic Materials (E 399) that thickness be greater than 2.5 K_{IC}^2/σ_{ys}^2.

After numerically analyzing a number of geometries, four basic coupons were selected to be used for generating an ERBS curves for PMMA. These included the half-dogbone tension coupon (HDT), the elongated compact-tension coupon (76.2 mm CT), the standard compact-tension coupon (CT), and the wide compact-tension coupon (CT-50.8 mm) (Fig. 2). The results of the numerical analysis (seen in Tables 1-4) show that testing of these geometries over a wide range of crack lengths can give fracture results which may be used for creating ERBS curves with B_E values ranging from -1.56 to +2.81. All results in these tables are for a unit applied load.

To evaluate the effectiveness of the ERBS curve for predicting failure in arbitrary coupons, various other specimen geometries were tested. These coupons include the single edge-notched coupon (SENT), the elongated compact-tension coupons (44.5 mm CT), and the delta coupons (DT=xx), seen in Fig. 3.

An MTS 880 test machine was used for the testing of all coupons. A clip gage was employed to measure the crack opening displacements (COD), and crack lengths were approximated through compliance equations. The load during precracking was continuously reduced to maintain a constant stress intensity factor, K_I.

In general the test procedures specified in ASTM E 399 were used to find K_C for each geometry. Most coupons were fatigue

precracked such that the maximum stress intensity of each cycle was less than 60% of the fracture toughness K_C for the last 2.5% of the precrack growth (as specified by ASTM E 399). Any test that exceeded this limit significantly was considered invalid. During fatigue precracking, the loading ratio was chosen to be 0.1, and the frequency was typically 30 Hz.

Just as in the ASTM E 399, the critical stress intensity K_Q was calculated for each coupon. If the test results for a particular coupon met the validity requirements, the K_Q value was considered to be the fracture toughness K_C. All plexiglas results met the ASTM E 399 requirement that P_M/P_Q should be less than 1.1.

For each coupon five crack length measurements were made as described in ASTM E 399 (c1 at the center, c2 and c3 at the midpoints between the surfaces and the center, and c4 and c5 on the surfaces). The crack length c, used for the analysis, was the average of the three inner measurements. According to ASTM E 399, for valid test results the crack front measurements must satisfy the following length, roundness, and symmetry requirements:

1. $0.45<c/W<0.55$
2. $\max(|c1-c2|,|c1-c3|,|c2-c3|)<0.1c$
3. $\min(c1,c2,c3,c4,c5)>(c+1.3\ mm)$
4. $\max(|c4-c|,|c5-c|)<0.15c$
5. $|c4-c5|<0.1c$

where W is the width of the coupon.

For this study, however, to obtain fracture results for a

wide range of B_E values, coupons with crack lengths shorter than c/W=0.45 and longer than c/W=0.55 were tested (contrary to requirement 1). As can be seen, guidelines 2, 4 and 5 are based on percentages of the crack length. These requirements are too restrictive for short cracks and too loose for long cracks for coupons of the same geometry. For example, consider requirement 2 which states that the maximum difference between any two of the inner crack length measurements must be less than 10% of the average crack length. For a short crack, c=5 mm, the maximum allowable difference would be 0.5 mm, whereas for a long crack, c=20 mm, this maximum allowable difference would be 2 mm. It is recognized that these requirements are adequate for the restricted crack lengths required by ASTM E 399. However, if coupons with longer and shorter cracks are to be tested it is recommended that the requirements be changed to be based on the fixed width of the coupon and not on the variable crack length. This would make the requirements equal for small and large cracks in coupons of the same geometry. For this study, the test was considered valid if the differences in guidelines 2, 4 and 5 were less than 0.1(W/2), 0.15(W/2), and 0.1(W/2) respectively.

Both K_I and the constant term T for each coupon were calculated using a modification of a numerical code written by Raju and Fichter [6]. The accuracy of this code was demonstrated in [4]. From the numerical work, K_C and B_E were determined for each coupon geometry. In this study c^* was chosen to be 25.4 mm as described in [4].

Experimental Results

The results of the experimental test program for PMMA will be presented using two different approaches. First, to demonstrate the limitations of the LEFM theory, the data will be analyzed using the assumption that K_{IC} is a material constant. Next, the ERBS failure criterion will be presented and analyzed. To illustrate the similarities and differences between both theories, each fracture model will be discussed in detail.

LEFM

Assume that an accurate prediction of fracture toughness is required for the coupon geometries (with a range of crack lengths) seen in Figs. 2-3 . These coupons, constructed of 12.7 mm thick PMMA, fulfill the LEFM requirements for brittle plane strain fracture (as pointed out earlier). Therefore, according to LEFM, failure should be predicted by a constant K_{IC}, independent of crack length and geometry.

To find K_{IC}, several tests were conducted using the guidelines specified in ASTM E 399. For each test a critical load P_Q was found. This load (and the coupon geometry) was used to determine the critical stress intensity factor K_Q. If the test conformed to the validity requirements specified in the standard, K_Q was then considered to be an accurate measure of the fracture toughness K_{IC}. For this study the fracture toughness of PMMA was found to be 1.018 MPa$\sqrt{m}$ (from fracture tests using CT coupons).

To evaluate the LEFM prediction that all planar PMMA cracked

bodies of the same thickness should fail at K_{IC}= 1.018 MPa$\sqrt{m}$, coupons of the geometries in Figs. 2-3 were next tested. The results of the tests are plotted in Fig. 4, where the horizontal line represents the predicted fracture toughness (1.018 MPa$\sqrt{m}$). Note the wide amount of scatter in the data. There is over 35% difference between the highest and lowest measured fracture toughness values. Some extreme cases of error in the failure predictions may be seen in the HDT and the SENT coupons. The HDT coupons have errors ranging from 23% below to 13% above the predicted K_{IC}. The fracture toughness of the SENT coupons is 15% higher than the predicted toughness.

A statistical analysis of the results shows that the standard deviation (or standard error) is σ = 0.110 MPa$\sqrt{m}$. By using the Student t distribution it can be shown that the test results have a 95% confidence level within a range of ±0.181 MPa$\sqrt{m}$ from the predicted value. This means that the LEFM K_{IC} approach predicts fracture 95% of the time to within ±18% error for this material.

Note that a wide range of crack lengths were tested for each coupon, this explains why there is so much scatter in the data. For the characterization of K_{IC}, ASTM E 399 restricts the crack length to fall with the range $0.45<c/W<0.55$. If tests were conducted on the geometries specified above with such a limited range of crack lengths, the scatter would not be as large.

It is interesting to note that during fracture of the CT-50.8 mm coupons, the crack initially propagated at a small angle from the horizontal ($0^{\circ}<\alpha<5^{\circ}$, see Fig 5). As fracture progressed

in the these coupons the crack continued to turn until arm breakage occurred. This initial small angle crack turning was also noted in some CT and DT coupons. The arm breakage was, however, found exclusively in the CT-50.8 mm coupons. These differences in crack propagation direction cannot be predicted by the single parameter K_{IC}.

ERBS

Now consider the ERBS approach for predicting failure in the PMMA coupons of Fig. 3. To make such predictions it was necessary to generate the ERBS curve for PMMA. This required the testing of various coupons of different geometry (as opposed to one coupon geometry for LEFM). For this study, the specimens shown in Fig. 2, with a wide range of crack lengths, were chosen. These coupons gave fracture results for $-0.57<B_E<2.81$. Each fracture test represented only one point on the ERBS curve. Polynomial curve fits were made to the data to give a mathematical expression for the ERBS curve.

The tests were conducted following the procedures specified by ASTM E 399 for K_{IC} determination; however, nonstandard coupons were used, and the crack front validity requirements were altered as discussed in the previous section. From each test, a load vs. COD curve was obtained, and the critical load P_Q was determined. If the results from a particular test were valid, K_Q was considered to be the fracture toughness, K_C, for the ERBS ratio B_E corresponding to the particular coupon geometry.

For clarity, first consider the test results of the HDT and

the 76.2 mm CT coupons shown in Fig. 6. This region of the ERBS curve will be called Zone I. As seen in the figure, a second order polynomial curve fits closely to the data. A statistical analysis shows that a polynomial of this order gives the best fit to the data (the standard error, σ, is minimum).

Now consider the fracture results of the CT-50.8 mm coupons shown in Fig. 7. This part of the ERBS curve will be called Zone III. There are two points that seem to indicate that the failure mechanism in Zone III is different from that in Zone I. First, as seen in the figure, the shape of the ERBS curve within Zone I is dramatically different from the shape of the curve inside Zone III. Second, the crack propagation direction appears to be different. Apparently a crack turning fracture mechanism occurs in Zone III, while Zone I exhibits a more stable transverse crack growth mechanism. Within Zone III the critical stress intensity K_C (because of crack branching K_C is not referred to as the fracture toughness) appears to be nearly constant (1.160 MPa$\sqrt{m}$). Therefore, an approach similar to that of LEFM for predicting fracture behavior may be used within this zone, however a proper K_{IC} must be found. Obviously the fracture results from coupons geometries of another zone may not be accurate as seen in Fig. 4 (1.160 MPa$\sqrt{m}$ is much more accurate than the results from the CT coupon testing, 1.018 MPa$\sqrt{m}$).

Zone II seems to be a transitional region between Zone I and Zone III. This region is determined by the fracture results of the standard CT coupon (see in Fig. 10). Within this zone there is a considerable amount of scatter in the fracture results. It

is interesting to note that small amounts of crack turning were seen in some, but not all of these coupons. The failure of coupons within Zone II may be predicted by an average critical stress intensity of 1.100 MPa$\sqrt{m}$.

These results support the conclusions of Betegon and Hancock [7] that J_{IC} may be influenced by the constant term, within the region $T<0$ ($B_E<1$). Note that Zone I falls within this region. They also hypothesized that J_{IC} would be nearly constant for $T>0$ ($B_E>1$). This behavior was seen in Zone III. Betegon and Hancock did not present any experimental work to verify their predictions.

With the characterization of the fracture behavior of PMMA through the ERBS curve, the failure in the coupons of Fig. 3 could be predicted. To do so, the stress intensity factor K_I and the constant term T for each coupon geometry were determined numerically. From these parameters, B_E was calculated using equation 1. The fracture toughness, K_C, for each B_E value was read from the ERBS curve. It was predicted that failure, in these coupons, would initiate when K_I reached this critical stress intensity factor, K_C. The major differences between this method for predicting fracture from the LEFM approach is that B_E is calculated and that the fracture toughness K_C is not a constant but changes with B_E.

When analyzed numerically it was found that the SENT coupons and the 44.5 mm CT coupons have B_E values which fall within Zone I. The results of the fracture tests for these coupons are plotted in Fig. 8 along with the ERBS curve for Zone I. Note how

closely the data fit the ERBS curve. The maximum percent error is 7% for one SENT coupon. All other results have error below 5.5%.

A statistical analysis for this zone determined that the standard error for this prediction is σ = 0.0362 MPa$\sqrt{m}$. This can be interpreted statistically to say that 95% of all Zone I fracture toughness test results will be predicted by the ERBS curve to within 6% error. The region of 95% confidence for the ERBS approach is nearly three times smaller than that for the LEFM method.

The DT=6.4 mm and DT=12.7 mm coupons have B_E values which fall within Zone III (see Fig. 9). The maximum percent error is 6%. Statistically the ERBS theory predicts the critical stress intesity factors within this region with the same amount of accuracy as seen in Zone I. As expected, these coupons exhibit small amounts of crack turning at initiation as did the CT-50.8 mm coupons.

The DT=25.4 mm coupons fall within Zone II. Because of the scatter in this region the accuracy of the ERBS theory, within this zone, is little better than that of the LEFM approach. Fig. 9 is a plot of the complete ERBS curve along with all the fracture data. This figure clearly shows the transitional zone.

As can be seen from the results presented above, through the use of the ERBS curve, one can predict fracture behavior in PMMA more accurately than with the LEFM K_{IC} approach (except within Zone II where they are nearly equal). Also, it seems that the curve may be used to predict the initiation of crack turning

(Zone III). It should be noted that most of the testing procedures and many of the numerical analyses are simple extensions to the current LEFM approach.

It is interesting to note that the crack path stability criterion proposed by Cotterell [8] is not completely accurate for the coupons tested in this study. It is true that for values of $T<0.0$ ($B_E<1.0$) that no branching (Class I fracture) occurs. However for $T>0.0$ ($B_E>1.0$) branching (Class II fracture) does not always occur. This is illustrated by the fracture behavior of the 76.2 mm CT specimens. These coupons exhibited no branching behavior though in most cases B_E was greater than 1.0 ($T>0.0$).

Conclusions

It has been clearly demonstrated through the experimental results of this study that the LEFM assumption that fracture toughness is a constant material property may lead to inaccurate predictions of fracture behavior. As seen in the testing results, K_C can be strongly dependent on the geometry of a cracked body. Also, the LEFM approach cannot be used to predict differences in crack propagation direction at initiation.

This study has shown that the ERBS curve predicts fracture initiation with a 95% confidence zone that is nearly three times smaller than that of the LEFM approach. The experimental results also show that the theory does predict changes in fracture behavior due to differences in geometry. The ERBS concept also has the potential to predict crack branching. A major advantage of this theory is that many of the procedures and methods of

analysis are the same as those used in the LEFM method.

Because the ERBS theory can account for differences in fracture behavior, these results verify the conclusions of various researchers, summarized by Eftis et. al. [1], that the T stress plays a significant role in fracture. The experimental results have also shown that the crack path direction stability criterion suggested by Cotterell [8] may not be accurate in all cases.

References

[1] Eftis, J., Jones, D. L., and Liebowitz, H., "Load Biaxiality and Fracture: Synthesis and Summary," Engineering Fracture Mechanics, Vol. 36, No. 4, 1990, pp. 537-574.

[2] Kibler, J. J., and Roberts, R., "The Effect of Biaxial Stresses on Fatigue and Fracture," Journal of Engineering for Industry, Vol 92, Nov. 1970, pp 727-734.

[3] Albritton, J. R., and Goree, J. G., "Fracture of Silicon Carbide Whisker Reinforced Aluminum," Proceedings of the 7th International Conference on Fracture (ICF7), 20-24 March 1989, pp. 889-896.

[4] Richardson, D. E., "A New Biaxial Stress Failure Criterion," Ph.D. thesis, Clemson University, August 1991.

[5] Wu, E. M., "Fracture Mechanics of Anisotropic Plates, Composite Material Workshop, Technomic Publishing Co. Inc., Lancaster, Pennsylvania, 1968, pp. 20-43.

[6] Raju, I. S., and Fichter, W. B., A Finite-Element Alternating Method for Two Dimensional Mode I Crack Configurations. Engineering Fracture Mechanics, Vol. 33, No. 4, 1989, pp. 525-540.

[7] Betegon, C., and Hancock, J. W., "Two-Parameter Characterization of Elastic-Plastic Crack-Tip Fields," Journal of Applied Mechanics, Vol. 58, March 1991, pp. 104-110..

[8] Cotterell, B., "Notes on the Paths and Stability of Cracks," International Journal of Fracture Mechanics, **Vol. 13**, 1980, pp. 526-533.

TABLE 1--Numerical results for the HDT coupon.

Crack Length (mm)	K_I (MPa$\sqrt{m}$)	T (MPa)	B_E
5.6444	0.13033	-1.18194	-1.56441
6.3500	0.15825	-1.33618	-1.38765
7.7612	0.22429	-1.64921	-1.07926
9.1722	0.30225	-1.96480	-0.83818
10.5834	0.39867	-2.28238	-0.61883
11.9944	0.51105	-2.58969	-0.43292
12.7000	0.57496	-2.74090	-0.34801
14.8166	0.79819	-3.16687	-0.12190
15.8750	0.93305	-3.35393	-0.01644
16.9334	1.09308	-3.53321	0.08599
17.9916	1.28062	-3.68965	0.18530
19.0500	1.48455	-3.79873	0.27643
21.1666	2.02281	-3.89809	0.45508
22.2250	2.34955	-3.81376	0.54101
23.2834	2.77288	-3.64435	0.62836
24.3416	3.24088	-3.28312	0.71354
25.4000	3.86518	-2.73711	0.79976
26.8112	4.91022	-1.45940	0.91596
28.2222	6.34130	0.76555	1.03414
28.9278	7.23913	2.56218	1.10008

TABLE 2--Numerical results for the 76.2 mm CT coupon.

Crack Length (mm)	K_I (MPa$\sqrt{m}$)	T (MPa)	B_E
9.1722	3.3665	-4.09949	0.65566
10.5834	3.8699	-3.30567	0.75846
11.9944	4.4585	-2.34954	0.85099
12.7000	4.7875	-1.78884	0.89434
13.8544	5.4176	-0.71963	0.96244
15.5865	6.5019	1.35032	1.05873
16.7409	7.4254	3.14419	1.11974
17.8956	8.5501	5.43802	1.17985
19.0500	9.9321	8.41259	1.23951
20.2044	11.6741	12.38811	1.30007
21.9365	15.3615	21.20585	1.39035
23.0909	18.8228	30.45101	1.45746
24.2456	23.6158	44.31368	1.53060
25.4000	30.6717	66.96727	1.61739

TABLE 3--Numerical results for the CT coupon.

Crack Length (mm)	K_I (MPa$\sqrt{m}$)	T (MPa)	B_E
9.1722	3.6579	17.92279	2.38549
10.5834	4.2664	11.97951	1.79399
11.9944	5.0112	9.15973	1.51686
12.7000	5.4073	8.91255	1.46607
13.8544	6.0901	10.82356	1.50255
15.5865	7.3235	16.04473	1.61951
16.7409	8.2298	20.16374	1.69281
17.8956	9.2943	24.42892	1.74322
19.0500	10.5982	28.77470	1.76774
20.2044	12.2550	33.30189	1.76840
21.9365	15.8405	41.45598	1.74003
23.0909	19.3329	49.25306	1.72039
24.2456	24.2719	61.30503	1.71421
25.4000	31.7734	83.52465	1.74333

TABLE 4--Numerical results for the CT-50.8 mm coupon.

Crack Length (mm)	K_I (MPa$\sqrt{m}$)	T (MPa)	B_E
11.9944	4.6684	10.41614	1.63091
12.7000	4.9711	10.41476	1.59242
13.8544	5.4530	12.79540	1.66351
15.5865	6.2254	18.95601	1.86102
16.7409	6.6594	23.86884	2.01351
17.8956	7.0641	28.99782	2.16075
19.0500	7.4497	34.16783	2.29691
20.2044	7.8258	39.20276	2.41652
21.9365	8.4127	46.57400	2.56545
23.0909	8.8217	51.20131	2.64120
24.2456	9.2519	55.64975	2.70085
25.4000	9.6869	59.93216	2.74947
26.9113	10.2874	65.38004	2.79710
28.1686	10.8253	69.60158	2.81808

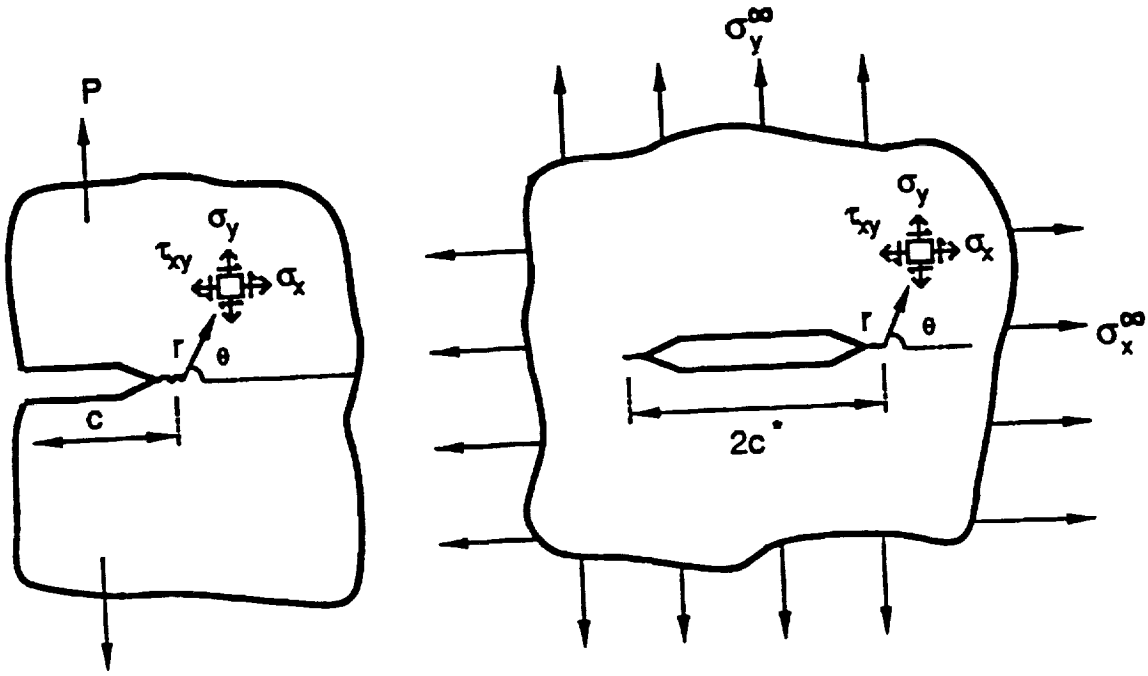

FIGURE 1. Comparison of an arbitrary cracked coupon with an infinite center-cracked panel.

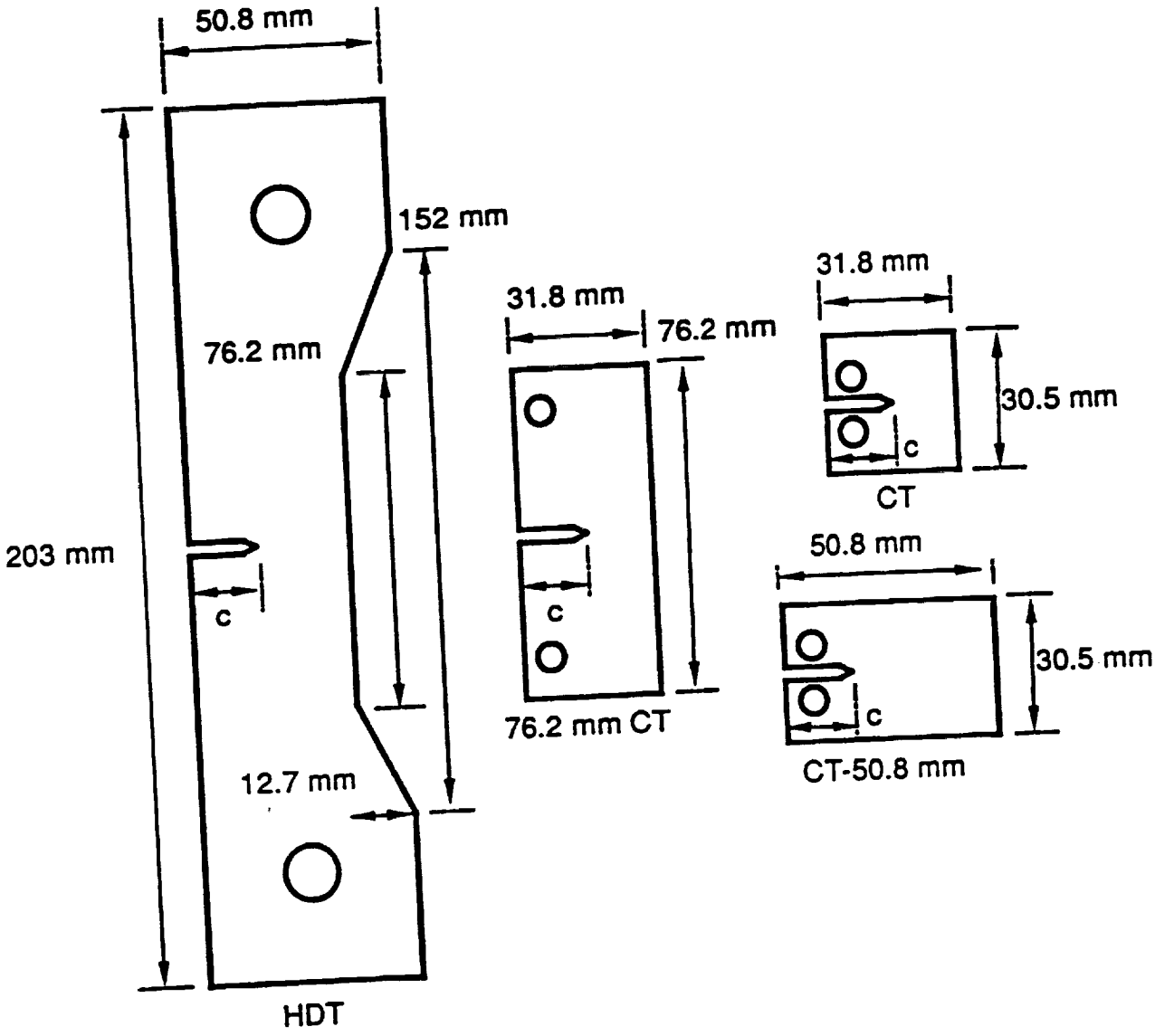

FIGURE 2. The four basic coupon geometries used in the test program (HDT, 3" CT, CT, and CT-2").

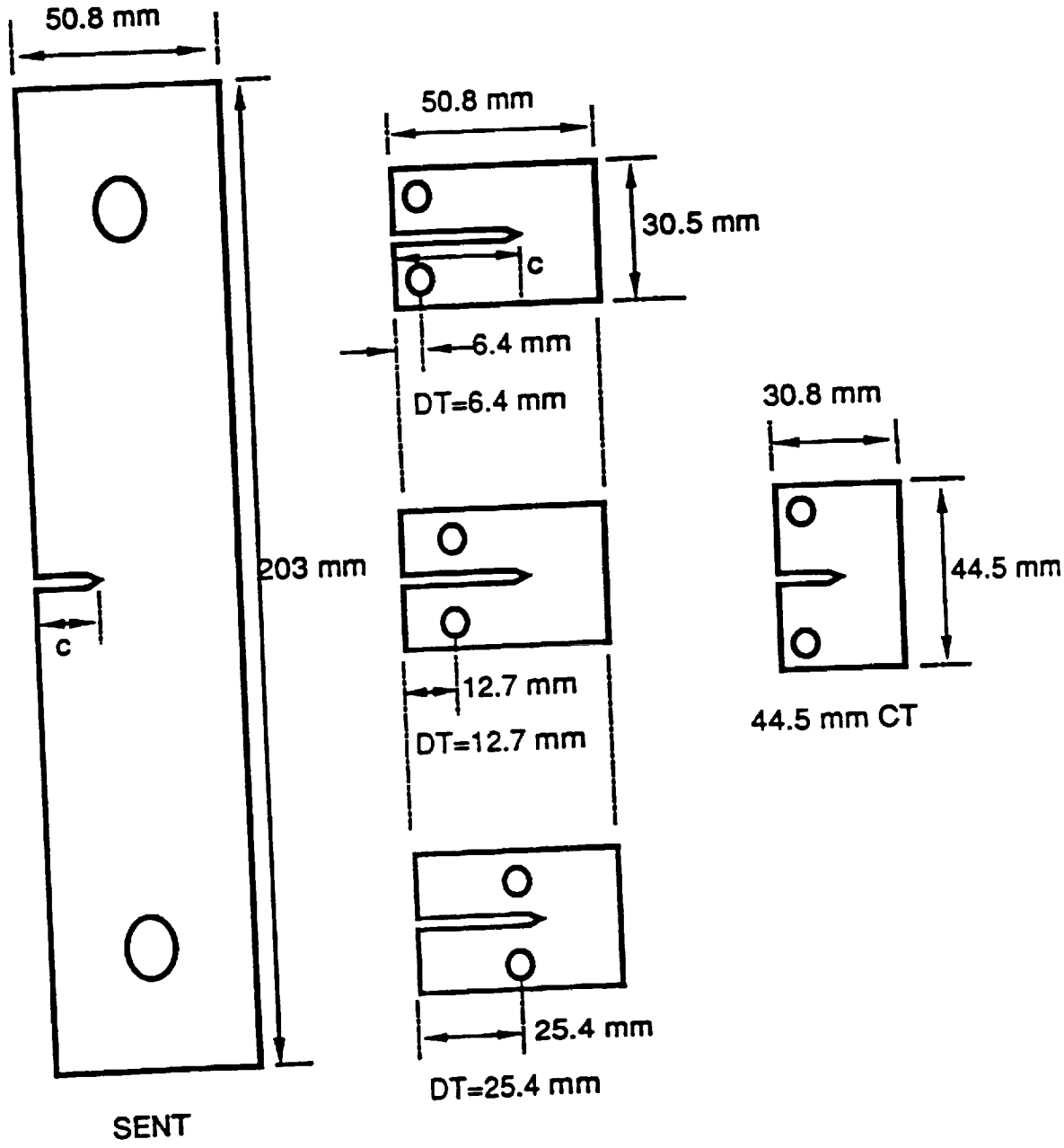

FIGURE 3. The SENT, DT=xx, and the CT 1.75" coupons.

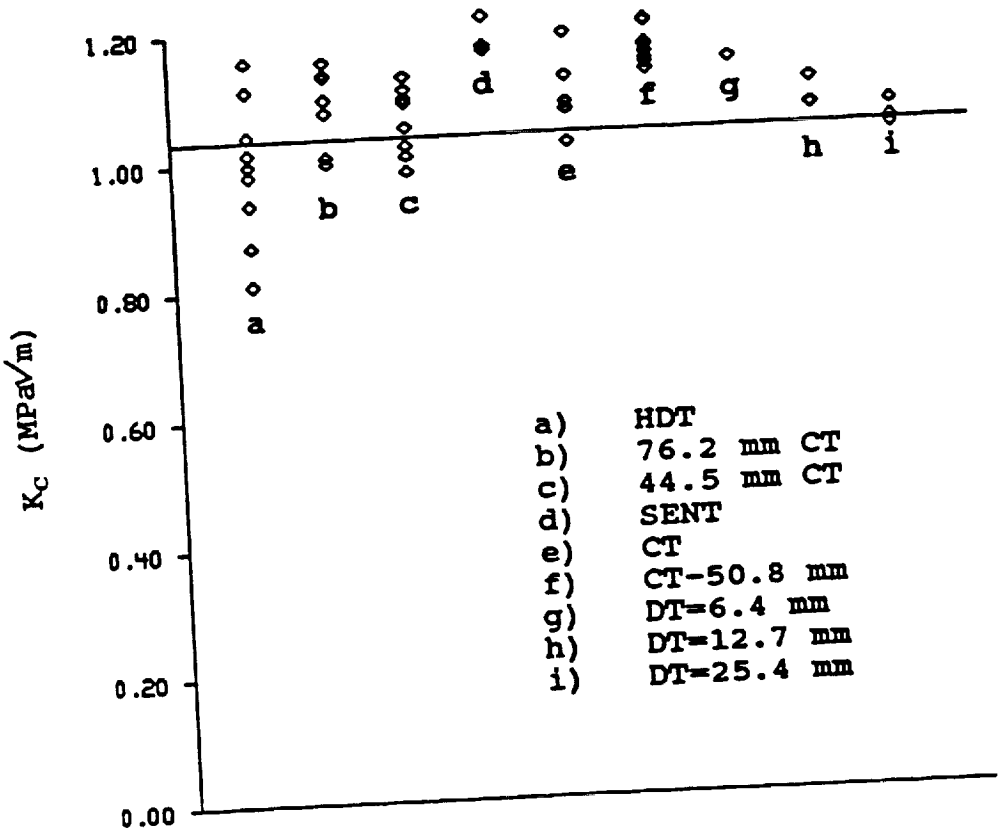

FIGURE 4. Fracture results of the PMMA coupons using the LEFM approach.

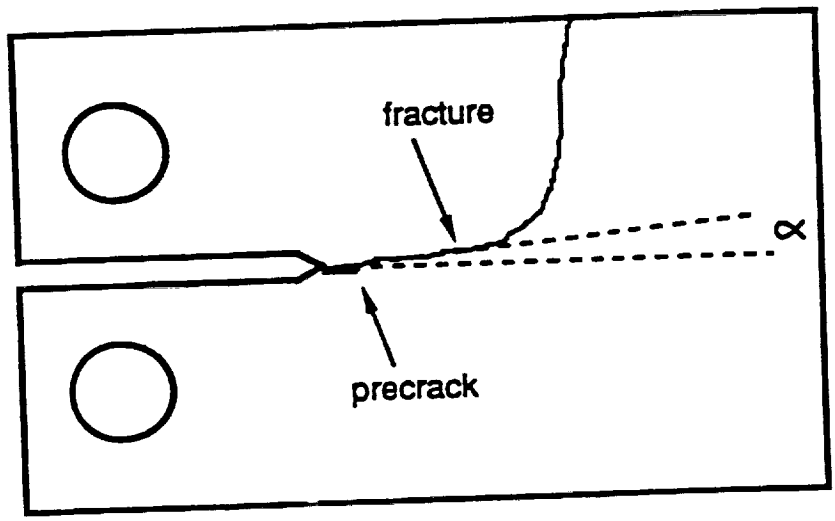

FIGURE 5. Crack turning in CT-2" coupons.

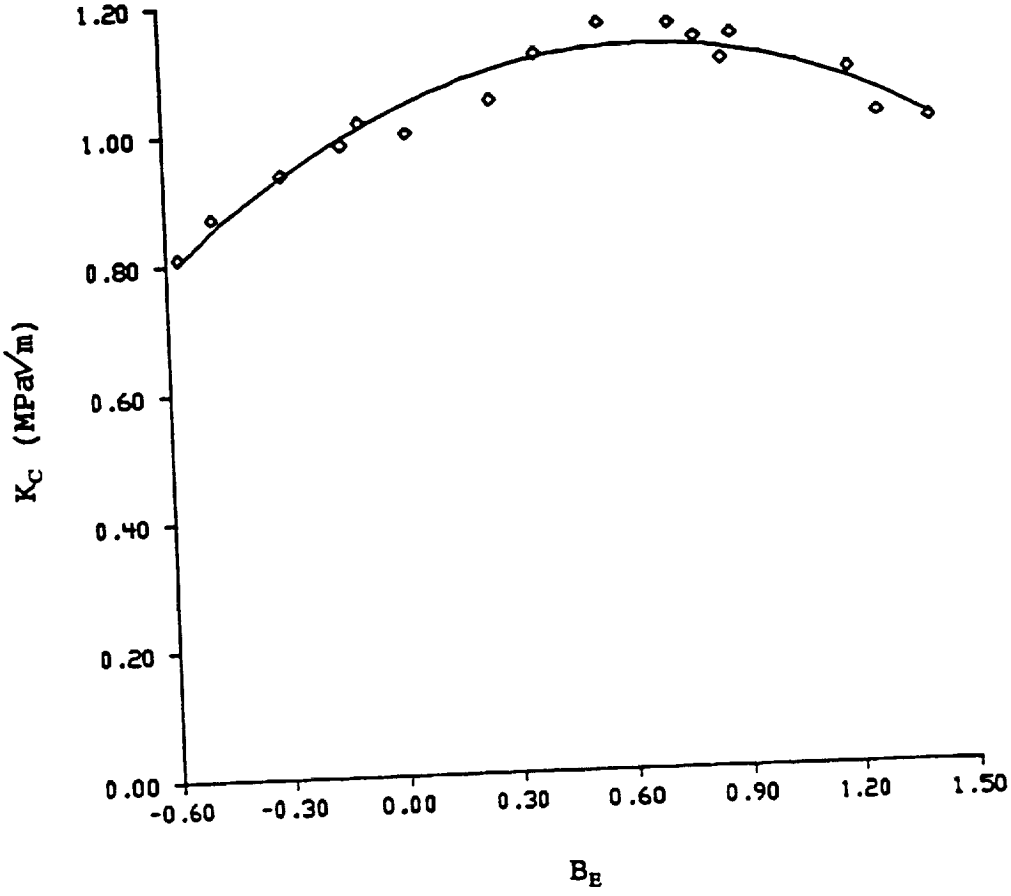

FIGURE 6. The Zone I ERBS curve for PMMA.

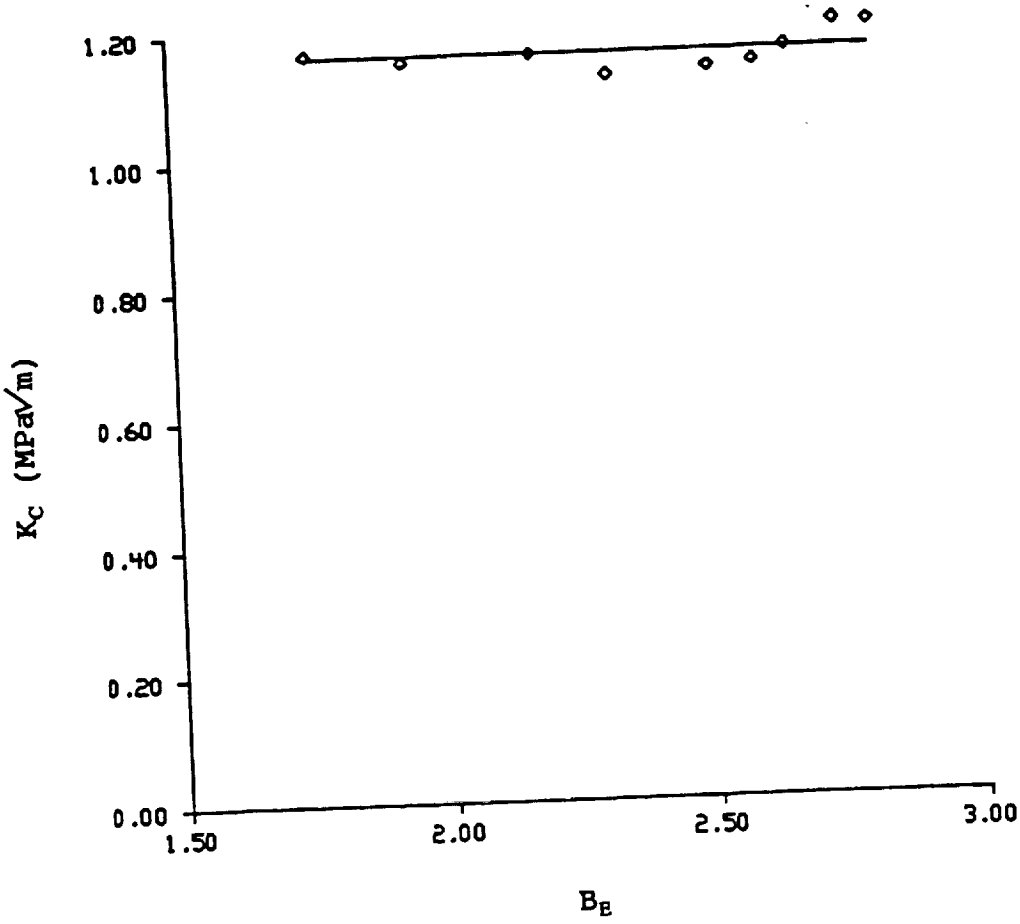

FIGURE 7. The Zone III ERBS curve for PMMA.

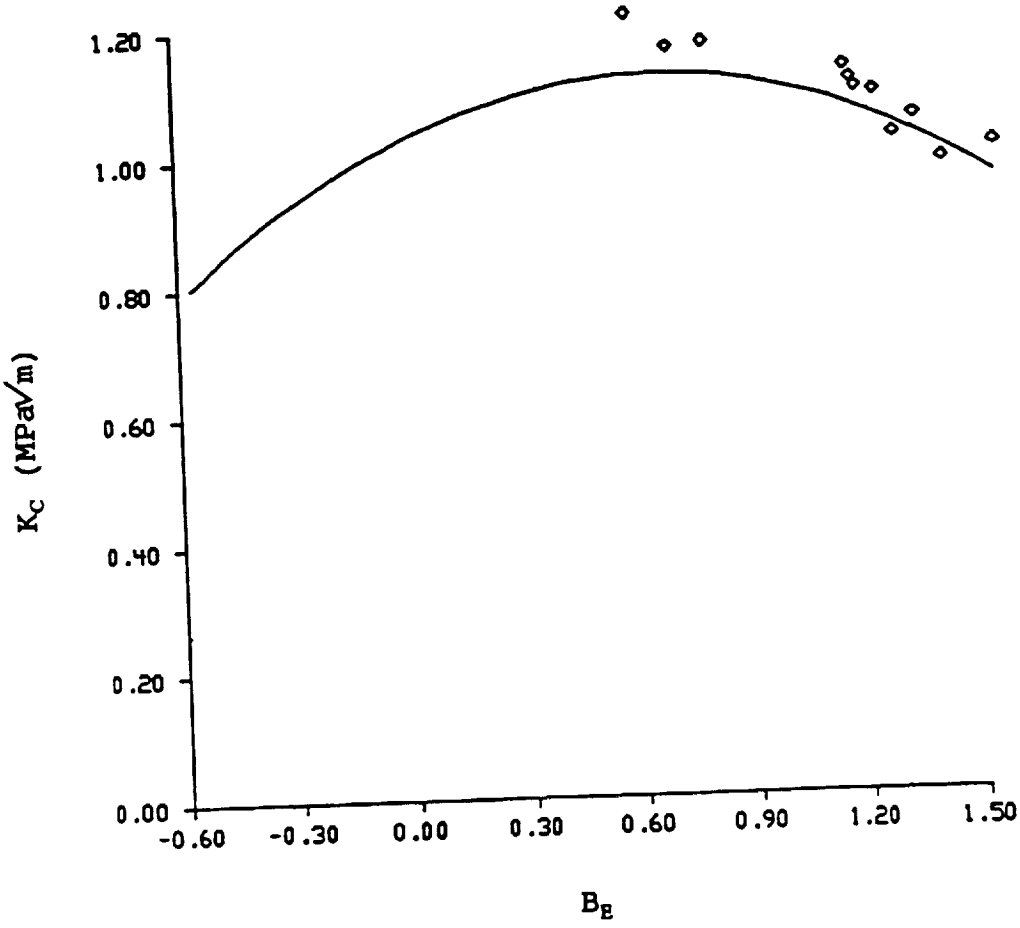

FIGURE 8. Fracture predictions within Zone I for PMMA.

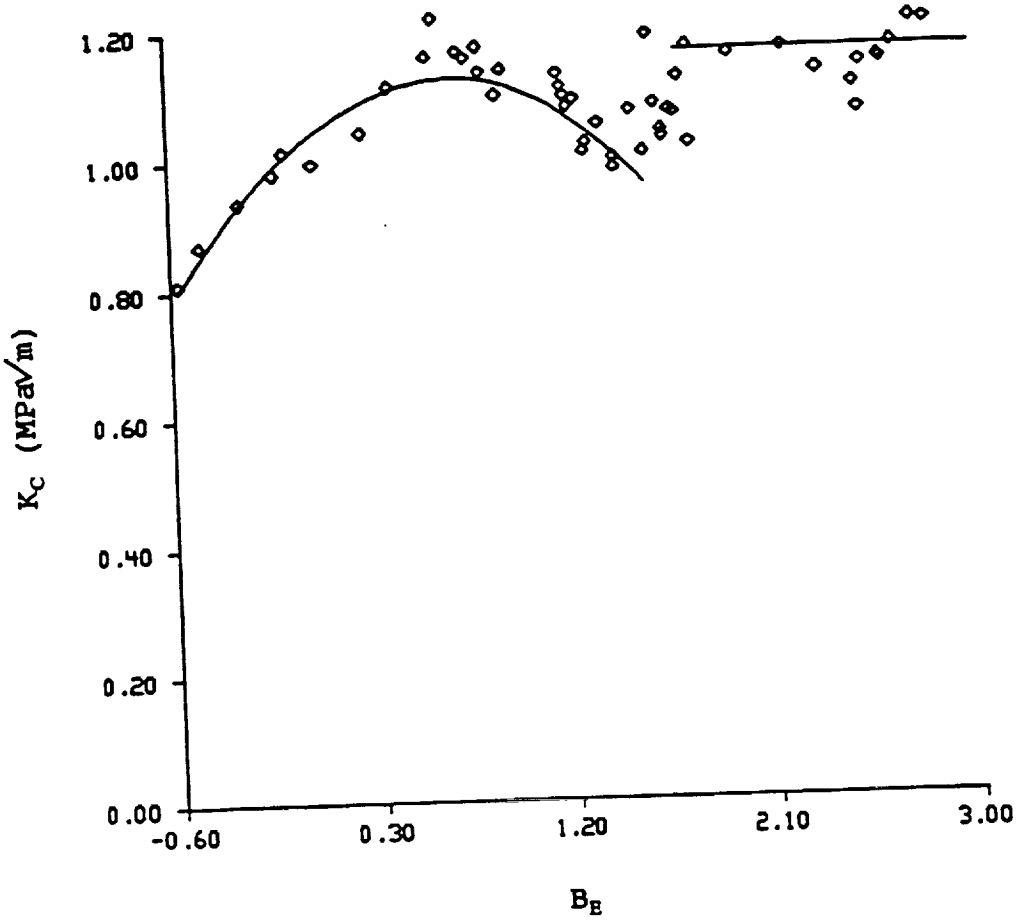

FIGURE 9. The complete ERBS curve and all PMMA fracture results.